

# Carbon nanotubes as multifunctional biological transporters and near-infrared agents for selective cancer cell destruction

Nadine Wong Shi Kam\*, Michael O'Connell\*, Jeffrey A. Wisdom†, and Hongjie Dai\*‡

\*Department of Chemistry and Laboratory for Advanced Materials, and †Department of Applied Physics, Stanford University, Stanford, CA 94305

Edited by Harry B. Gray, California Institute of Technology, Pasadena, CA, and approved June 30, 2005 (received for review April 1, 2005)

Biological systems are known to be highly transparent to 700- to 1,100-nm near-infrared (NIR) light. It is shown here that the strong optical absorbance of single-walled carbon nanotubes (SWNTs) in this special spectral window, an intrinsic property of SWNTs, can be used for optical stimulation of nanotubes inside living cells to afford multifunctional nanotube biological transporters. For oligonucleotides transported inside living cells by nanotubes, the oligos can translocate into cell nucleus upon endosomal rupture triggered by NIR laser pulses. Continuous NIR radiation can cause cell death because of excessive local heating of SWNT *in vitro*. Selective cancer cell destruction can be achieved by functionalization of SWNT with a folate moiety, selective internalization of SWNTs inside cells labeled with folate receptor tumor markers, and NIR-triggered cell death, without harming receptor-free normal cells. Thus, the transporting capabilities of carbon nanotubes combined with suitable functionalization chemistry and their intrinsic optical properties can lead to new classes of novel nanomaterials for drug delivery and cancer therapy.

cancer cells | optical excitation | radiation therapy | drug delivery  
nanobiotechnology

The introduction and delivery of DNA, proteins, or drug molecules into living cells is important to therapeutics (1). Inorganic nanomaterials, including nanocrystals, nanotubes, and nanowires, exhibit advanced physical properties promising for various biological applications (2–6), including new molecular transporters. Single-walled carbon nanotubes (SWNTs) have been shown to shuttle various cargoes across cellular membrane without cytotoxicity (7–9). Much remains to be done to exploit the intrinsic physical properties of SWNTs (10) and thus impart unique features to nanotube biocarriers. Here, we show that while biological systems are transparent to 700- to 1,100-nm near-infrared (NIR) light (11), the strong absorbance of SWNTs in this window (12) can be used for optical stimulation of nanotubes inside living cells to afford various useful functions. For oligonucleotides transported inside cells by nanotubes, the oligos can translocate into cell nucleus upon endosomal rupture triggered by NIR laser pulses. Continuous NIR radiation can cause cell death because of excessive local heating of SWNTs *in vitro*. Selective cell destruction can be achieved by functionalization of SWNTs with a folate moiety, selective internalization of SWNTs inside cells labeled with folate receptor (FR) tumor markers (13), and NIR-triggered cell death, without harming receptor-free normal cells. The intrinsic physical properties of SWNTs can thus be exploited to afford new types of biological transporters with useful functionalities.

## Materials and Methods

**Water-Soluble Cy3-DNA-SWNT Conjugates and Characterization.** As-grown Hipco (14) SWNTs were mixed with a 20- $\mu$ M aqueous solution of Cy3-labeled single-stranded DNA, and the initial concentration of SWNTs was  $\approx$ 250 mg/liter. The DNA sequence was TGGACAAGTGGAATGX, where X denoted the fluorescent label Cy3, and was purchased from the Stanford Protein and Nucleic Acid Biotechnology Facility. The nanotubes and DNA

solution were sonicated for  $\approx$ 45 min to 1 h and centrifuged at  $22,000 \times g$  for  $\approx$ 6 h. The pellet comprising of impurities, aggregates, and bundles of nanotubes at the bottom of the centrifuge tube was discarded, and the supernatant was collected and underwent an additional centrifugation round. The resulting supernatant consisted of a solution of SWNTs functionalized by Cy3-DNA by noncovalent adsorption (15). The solubilized SWNTs were mostly individual tubes (nonaggregated) and small bundles as revealed by spectroscopy and microscopy with a Cary 6000i UV-visible-NIR spectrophotometer and atomic force microscopy (AFM), respectively. The SWNT concentration in the solution after this process was estimated to be  $\approx$ 25 mg/liter ( $\approx$ 10% of the starting nanotube suspension). Samples for AFM analysis were prepared by depositing  $\approx$ 50  $\mu$ l of the SWNT suspension on a SiO<sub>2</sub> substrate and allowing it to stand for 45 min. The substrate was then thoroughly rinsed with distilled water and dried with a N<sub>2</sub> stream.

**SWNTs Functionalized by Various Phospholipids (PLs).** PLs with a polyethylene glycol (PEG) moiety and folic acid (FA) terminal group (PL-PEG-FA). FA (Aldrich) (3.5 mM) and 5 mM 1-ethyl-3-(3-dimethylamino-propyl) carbodiimide (EDC, Fluka) were added to a solution of 0.35 mM PL-PEG-NH<sub>2</sub> (2-distearoyl-*sn*-glycero-3-phosphoethanolamine-*N*-[amino(PEG)2000] purchased from Avanti Polar Lipids) in 10 mM phosphate buffer at pH 7.5. After reaction, the solution was dialyzed against phosphate buffer by using a membrane (molecular weight cutoff = 1,000) to remove unreacted FA and EDC. The dialysis was carried out for 3 days with frequent replacement of the buffer. After dialysis, the absorbance of the PL-PEG-FA solution was recorded with an HP-8453 spectrophotometer (Hewlett-Packard) to ensure that excess free FA was removed from the solution.

**PL with a PEG moiety and fluorescein tag (PL-PEG-FITC).** Three milligrams of PL-PEG-NH<sub>2</sub> was dissolved in 1.5 ml of 0.1 M carbonate buffer solution (pH 8.0). To this solution 100  $\mu$ l of 13 mM solution of FITC in DMSO (Aldrich) was added. The mixture was allowed to react overnight at room temperature and protected from light. Purification by gel chromatography was achieved by loading 1 ml of the solution to a Sephadex G-25 column (Aldrich). As elution solvent (H<sub>2</sub>O) was flown through the column the formation of two separate yellow bands was observed. The fractions were collected, and the absorbance of various fractions was measured at 488 nm with a HP-8453 spectrophotometer. Fractions from the first elution peak were pooled as they were attributed to the higher molecular weight PL-PEG-FITC conjugate (also confirmed by fluorescence measurement), and subsequently used for solubilization of SWNTs.

**Solutions of SWNTs Functionalized with One or Two PL-PEG Molecules (One or Two Cargoes).** PL-PEG-FA (one cargo, used in Fig. 5 *b* and *c*) or a 1:1 mixture of PL-PEG-FA and PL-PEG-FITC (two cargoes,

This paper was submitted directly (Track II) to the PNAS office.

Abbreviations: NIR, near-infrared; SWNT, single-walled carbon nanotube; AFM, atomic force microscopy; PL, phospholipid; PEG, polyethylene glycol; FA, folic acid; FR, folate receptor.

‡To whom correspondence should be addressed. E-mail: hdai@stanford.edu.

© 2005 by The National Academy of Sciences of the USA

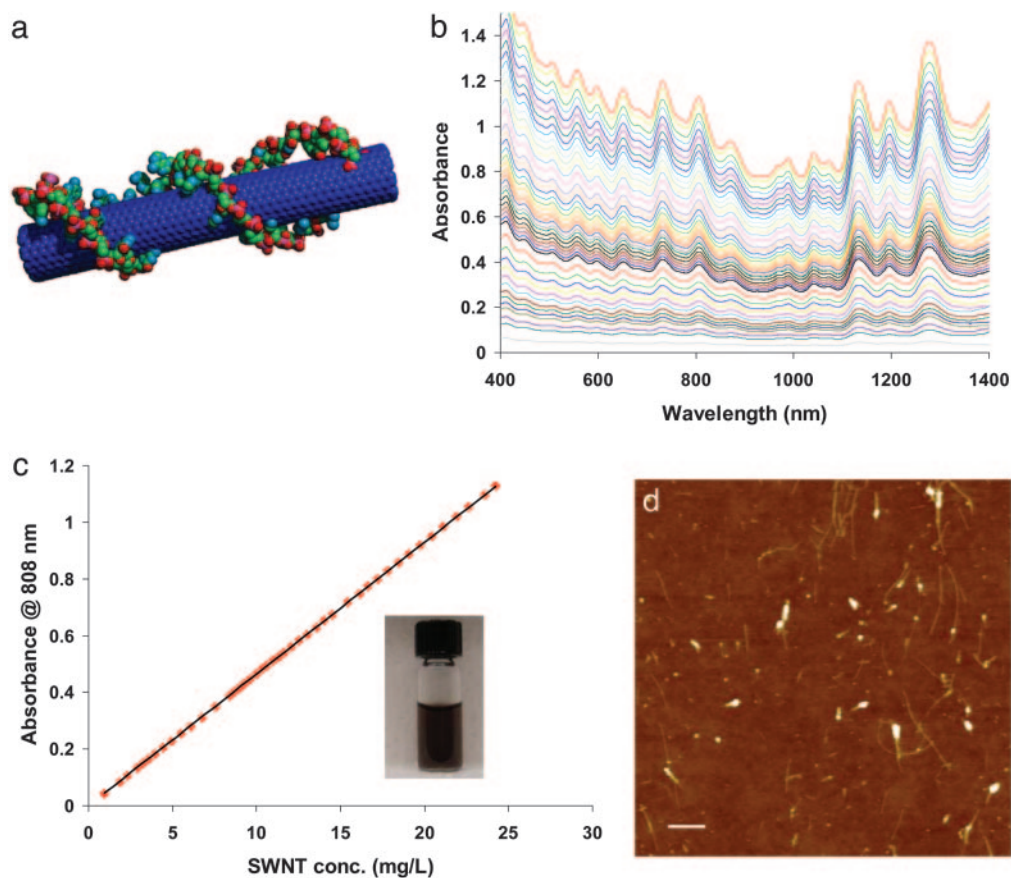


**Fig. 1.** Carbon nanotubes with high NIR absorbance solubilized in water. (a) Schematic of a Cy3-DNA-functionalized SWNT. The drawing is only a graphic presentation and does not represent the precise way DNA binds on SWNTs. (b) UV-visible spectra of solutions of individual SWNTs functionalized noncovalently by 15-mer Cy3 labeled-DNA at various nanotube concentrations (top curve, SWNT concentration  $\approx 25$  mg/liter in H<sub>2</sub>O; lower curves correspond to consecutive 3% reduction in SWNT concentration). The well defined peaks in the UV-visible spectra suggest lack of large aggregated SWNTs in the solution by removing bundles by centrifugation. (c) Absorbance at 808 nm vs. SWNT concentration (optical path = 1 cm). Solid line is Beer's law fit to obtain molar extinction coefficient of SWNT  $\epsilon \approx 7.9 \times 10^6$  M<sup>-1</sup>cm<sup>-1</sup>. (Inset) A photo of a DNA-functionalized SWNT solution. (d) AFM image of DNA-functionalized individual SWNTs (height of 1–10 nm) deposited on a SiO<sub>2</sub> substrate. (Scale bar: 200 nm.)

used for Fig. 5 *d* and *e*) were used to functionalize and solubilize Hipco SWNTs by using the same sonication and centrifuging procedure as described for Cy3-DNA above. The SWNTs functionalized by PL-PEG molecules were also individual and small bundles of tubes characterized by UV-visible-NIR spectroscopy and AFM.

The suspensions of SWNTs obtained by DNA and PL treatment above were all stable in water and physiological buffers for at least several days at room temperature without aggregating and precipitating out of the solution. We also tested the stability by heating up to 80°C (above the physiological temperature) and observed no aggregation. These results suggest strong and stable noncovalent absorption of the molecules on SWNT sidewalls.

**Cell Culture and Cellular Incubation in SWNT Solutions.** HeLa cells (an adherent cell line) were cultured in DMEM supplemented with 10% FBS and 1% penicillin-streptomycin (all reagents from Invitrogen). The incubations of Cy3-DNA-SWNT with HeLa cells were carried out (see Figs. 2–4) in 12-well plates, with the cells having been seeded for  $\approx 18$  h before incubation. Cy-DNA-SWNT was added to each well ( $\approx 4 \times 10^5$  cells per well) at a final concentration of  $\approx 2.5$ –5 mg/liter. The incubations were carried out at 37°C (except for low-temperature incubation, where the temperature was 4°C, see Fig. 2*c*) and in 5% CO<sub>2</sub> atmosphere for  $\approx 12$  h. After incubation, the cell medium was removed from the well, and the cells were washed and detached from the surface by the

addition of trypsin-EDTA solution (Invitrogen) for various characterization or laser radiation steps. Similar steps were used for incubating cells in PL-PEG-functionalized SWNTs (see Fig. 5). Note that all cells were washed with excess SWNTs in the solution removed and placed in fresh solutions after the incubation step and before any of the *in vitro* laser radiation experiments described in this work.

**FR<sup>+</sup> Cells and Normal Cells.** HeLa cells were cultured in DMEM with FA depleted from the cell medium. It is known that the FA-starved cells overexpress FRs on the cell surfaces. HeLa cells were passaged for at least four rounds in the FA-free medium before use to ensure overexpression of FR on the surface of the cells (FR<sup>+</sup> cells). Normal cells were cultured in DMEM with abundant FA to give few available free FRs on the cell surfaces.

**808-nm Laser Radiation.** Detached HeLa cells with or without incubation treatment in SWNT solutions were transferred to a circular quartz cuvette (diameter of 3 cm, thickness or optical path length of 1 cm) and exposed to an 808-nm laser source, a fiber-coupled diode laser bar. Note that all cells were washed with excess SWNTs in the solution removed and placed in fresh solutions after incubation in SWNT solutions and before any of the *in vitro* laser radiation experiments described in this work. The diode laser bar was coupled into a 1-m long, 200- $\mu$ m core fiber with a numerical aperture of 0.22. The bare fiber end was imaged to the size of the



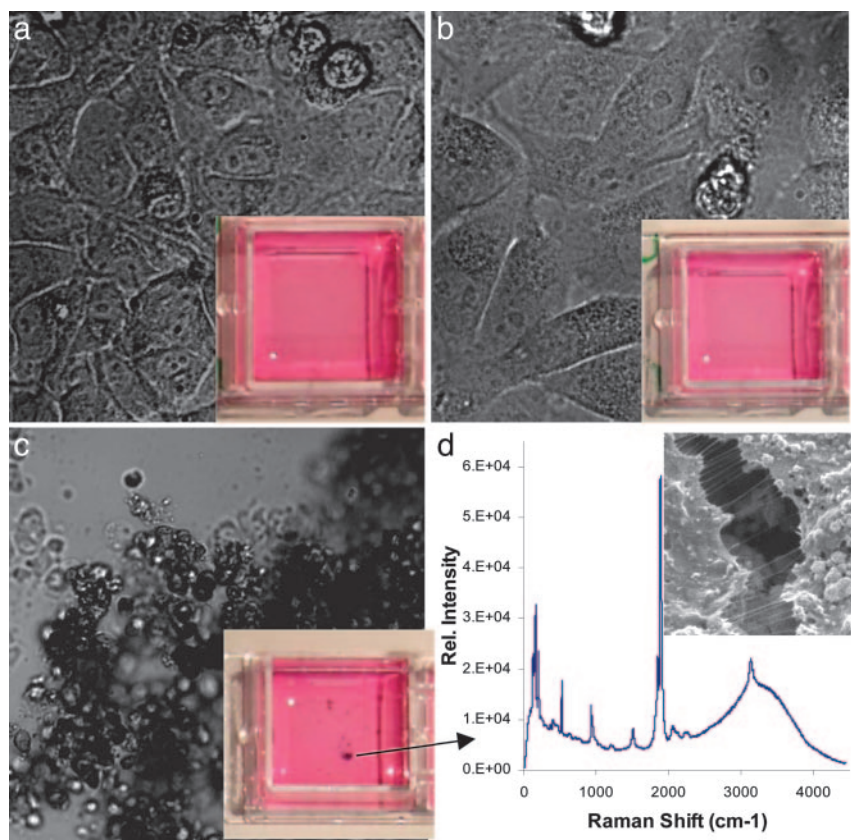


**Fig. 4.** Fate of cells with internalized SWNTs after NIR laser pulses or extensive radiations. (a) Optical image of HeLa cells after DNA-SWNT uptake and six pulses of 10-s, 808-nm laser radiations at 1.4 W/cm<sup>2</sup>. Cells retained normal morphology with no apparent death observed. (Inset) Photo of the cell solution taken 12 h after laser pulses. Pink color was caused by phenol red in the well. HeLa cells remained adhered to the bottom of the container. (b) Image of HeLa cells without internalized SWNTs after continuous 808-nm laser radiation at 3.5 W/cm<sup>2</sup> for 5 min. No cell death was observed. (Inset) Photo of cell solution after radiation. (c) Image of dead and aggregated cells after internalization of DNA-SWNT and laser radiation at 1.4 W/cm<sup>2</sup> for 2 min. The dead cells showed rounded morphology as opposed to live cells in a "stretched" form in a and b. (Inset) Photo of the cell solution 24 h after laser-activated cell death. No live cells adherent to the bottom of the container were observed. Black aggregates containing SWNTs released from dead cells floating on water were visible (indicated by arrow) to the naked eye. (d) Raman data and scanning electron microscopy image (Inset) of the black aggregates after drying. (Magnifications: ×20 for confocal images and ×36,000 for scanning electron microscopy.)

≈3.5 W/cm<sup>2</sup>, and the exposure was carried out either continuously for several minutes or over several 10-s pulses.

**Confocal Microscopy.** The cells were imaged by a Zeiss LSM 510 confocal microscope. Before analysis, the detached HeLa cells (with and without laser exposure) were seeded in chambered coverslides for ≈12 h. For nuclear staining, DRAQ5 (Axxora, Lausen, Switzerland) was added to each well and allowed to incubate for 5 min at room temperature before confocal imaging.

**Ex Vitro Measurement of Heating of a SWNT Solution by NIR Radiation.** A DNA-SWNT solution (nanotube concentration of 25 mg/liter) was irradiated by the 808-nm laser at 1.4 W/cm<sup>2</sup>. Temperature was measured (see Fig. 3c) at 20-s intervals with a thermocouple placed inside the solution for a total of 2 min. Care was taken to avoid exposure of the thermocouple in the beam path to minimize any direct heating of the thermocouple by the laser. Longer time radiation caused formation of gas bubbles in the solution and eventual boiling of the water solution, as a result of light absorption by SWNTs in the solution. Without nanotubes, an aqueous solution is transparent without heating under the same radiation conditions.

**Cell Proliferation Assay.** The CellTiter A96 (Promega) assay was used to monitor cell viability and proliferation after various treatments including internalization of SWNTs and laser radiation. The CellTiter A96 assay uses the tetrazolium compound [3-(4,5-dimethylthiazol-2-yl)-5-(3-carboxymethoxyphenyl)-2-(4-sulfophenyl)-2H-tetrazolium, inner salt; MTS] and the electron coupling reagent phenazine methosulfate. MTS is chemically reduced by cells into formazan whose concentration and optical absorbance at 490 nm can provide a measure of the metabolically active live cells.

Control cells or cells treated with SWNTs and/or laser treatment were left to incubate for up to 15 days at 37°C and 5% CO<sub>2</sub> in DMEM. The CellTiter A96 solution was added to each cell sample

and allowed to react for 2 h at 37°C and 5% CO<sub>2</sub>. Colorimetric detection and absorbance at 490 nm were used to determine the proliferation profile of different samples.

## Results and Discussion

The nanotube samples used here were Hipco SWNTs (14) solubilized in the aqueous phase by noncovalently adsorbing either 15-mer fluorescently Cy3-labeled single-stranded DNA (15) (Fig. 1a) or PEG-grafted PLs (PL-PEG) (see Fig. 5a). These nanotube solutions were highly stable in buffer solutions (Fig. 1c Inset), consisting of very pure, short (average length ≈150 nm, relatively straight because of short length) SWNTs by sonication and centrifugation (12) rather than large aggregates as evidenced by UV-visible-NIR absorbance (Fig. 1b) and AFM (Fig. 1d) data. The molar extinction coefficient of the solubilized SWNTs (molecular mass ≈170 kDa for length ≈150 nm, diameter ≈1.2 nm) measured at λ of 808 nm in the NIR was  $\epsilon \approx 7.9 \times 10^6 \text{ M}^{-1}\text{cm}^{-1}$  (Fig. 1c). The high absorbance of SWNTs in the NIR originates from electronic transitions between the first or second van Hove singularities of the nanotubes (12, 16). High optical absorbance of SWNTs in the 700- to 1,100-nm NIR window transparent to biological systems (11) is exploited in the current work at a single wavelength by using an 808-nm laser (beam size of ≈3 cm and power density up to 3.5 W/cm<sup>2</sup>) for *in vitro* radiation.

By confocal fluorescence microscopy imaging, we observed that upon exposure of HeLa cells to a Cy3-DNA-SWNT solution at 37°C the DNA-SWNT conjugates were internalized (Fig. 2 a and b) inside the cells with nanotubes as the transporters. The green color in Fig. 2a corresponds to Cy3 labels on DNA-SWNTs inside HeLa cells. After staining the cell nucleus with a DRAQ5 dye, we carried out dual color detection and observed accumulation of DNA-SWNT in the cytoplasm region with little colocalization of Cy3-DNA in the nucleus (Fig. 2b). This suggested lack of nuclear translocation for the DNA molecules transported across the cell

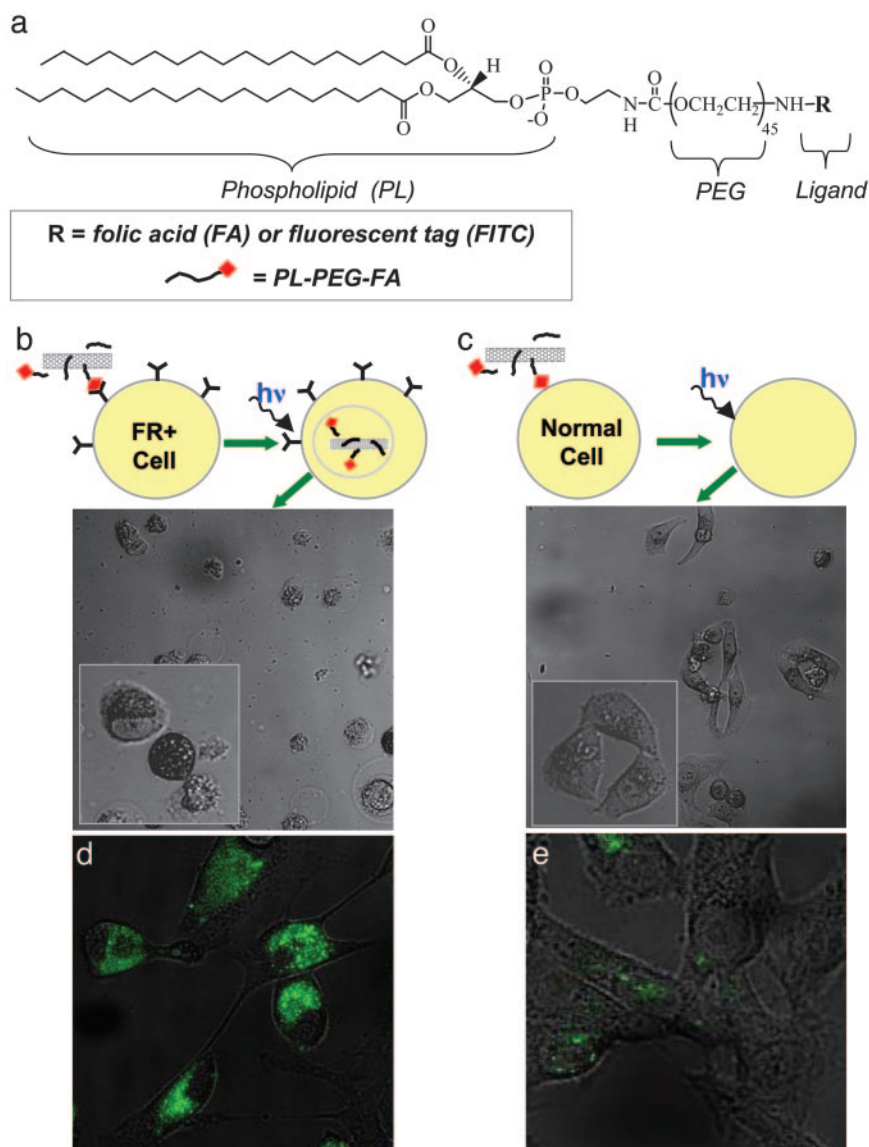


**Fig. 5.** Selective targeting and killing of cancer cells. (a) Chemical structure of PL-PEG-FA and PL-PEG-FITC synthesized by conjugating PL-PEG-NH<sub>2</sub> with FA or FITC, respectively, for solubilizing individual SWNTs. (b) (Upper) Schematic of selective internalization of PL-PEG-FA-SWNTs into folate-overexpressing (FR<sup>+</sup>) cells via receptor binding and then NIR 808-nm laser radiation. (Lower) Image showing death of FR<sup>+</sup> cells with rounded cell morphology after the process in Upper (808-nm laser radiation at 1.4 W/cm<sup>2</sup> for 2 min). (Inset) Higher-magnification image shows details of the killed cells. (c) (Upper) Schematic of no internalization of PL-PEG-FA-SWNTs into normal cells without available FRs. (Lower) Image showing normal cells with no internalized SWNTs are unharmed by the same laser radiation condition as in b. (Inset) Higher magnification image shows a live normal cell in stretched shape. (d) Confocal image of FR<sup>+</sup> cells after incubation in a solution of SWNTs with two cargoes (PL-PEG-FA and PL-PEG-FITC). The strong green FITC fluorescence inside cells confirms the SWNT uptake with FA and FITC cargoes. (e) The same as d for normal cells without abundant FRs on cell surfaces. There is little green fluorescence inside cells, confirming little uptake of SWNTs with FA and FITC cargoes. (Magnifications: ×20.)

membranes by nanotubes. Experiments carried out at 4°C found no uptake of Cy3-DNA-SWNT conjugates inside cells (Fig. 2c), suggesting an energy-dependent endocytosis mechanism (17) for the uptake observed at 37°C.

Endocytosis is known to rely on enclosure of molecules inside endosomes or lipid vesicles during and after cell entry (17). Motivated by the need of endosomal rupture for efficient molecular releasing and delivery (18), we explored the effects of NIR light on DNA-SWNTs after endocytosis. We first note that control experiments found that cells without nanotubes are highly transparent to NIR and exhibit no ill effect after radiation for up to 5 min by a 3.5 W/cm<sup>2</sup> ( $\lambda$  of 808 nm) coherent laser light (laser beam diameter of  $\approx$ 3 cm uniformly radiating over the entire area of the cuvette containing the cells). For HeLa cells after DNA-SWNT uptake, we experimented with the NIR radiation conditions and found that six 10-s on-and-off pulses of 1.4 W/cm<sup>2</sup> laser radiation can afford releasing effects without causing cell death. After such treatment, confocal imaging reveals colocalization of fluorescence of Cy3-DNA in the cell nucleus (Fig. 3a), indicating releasing of DNA cargoes from SWNT transporters and nuclear translocation after the laser pulses.

To glean the effects of NIR optical excitation of SWNTs inside living cells, we carried out a control experiment by radiating an

aqueous solution of Cy3-DNA-functionalized SWNTs *ex vitro*. We observed that radiation of a SWNT aqueous solution (nanotube concentration of 25 mg/liter) by 1.4 W/cm<sup>2</sup> ( $\lambda$  = 808 nm) laser continuously for 2 min caused heating of the solution to  $\approx$ 70°C (Fig. 3c, boiling of solution was observed for even longer radiations). Without solubilized nanotubes, the solution was transparent to 808-nm light with little heating detected. These findings clearly showed that optically stimulated electronic excitations of SWNTs rapidly transferred to molecular vibration energies and caused heating. Another phenomenon was that after *ex vitro* NIR radiation of a Cy3-DNA/SWNT solution (without cells), an apparent increase in the Cy3 fluorescence was observed (Fig. 3b), indicating unwrapping and releasing of Cy3-DNA strands from nanotubes and thus reduced quenching of Cy3 by nanotubes. Taken together, the results suggest that SWNTs internalized in living cells can act as tiny NIR “heaters” or “antennas.” Optoelectronic excitations of nanotubes inside cells by NIR radiation can trigger endosomal rupture and releasing of noncovalent molecular cargoes from nanotube carriers. Once detached from nanotubes and freed into the cytoplasm, the DNA molecules diffuse freely across the nuclear membrane (19) into the nucleus.

No apparent adverse toxicity effects were observed with cells after SWNT endocytosis and NIR pulse (1.4 W/cm<sup>2</sup>) activated

DNA releasing and nuclear translocation in terms of short-term viability (Fig. 4*a* and Fig. 6, which is published as supporting information on the PNAS web site) and long-term cell proliferation (Fig. 6). In a control experiment, cells without exposure to SWNTs survived continuous 3.5 W/cm<sup>2</sup>, 808-nm laser radiation for 5 min (Fig. 4*b*), clearly illustrating high transparency of biosystems to NIR light. In stark contrast, for cells with internalized SWNTs, extensive cell death was observed after 2 min of radiation under a 1.4 W/cm<sup>2</sup> power as evidenced by cell morphology changes (Fig. 4*c* vs. *a* and *b*), loss of adherence to substrates, and aggregation of cell debris (Fig. 4*c*). Extensive local heating of SWNTs inside living cells caused by continuous NIR absorption was the most likely origin of cell death. Interestingly, we observed that the dead cells “released” SWNTs to form black aggregates floating in the cell medium solution visible to the naked eye ≈24 h after irradiation (Fig. 4*c* *Inset*, black specks). Raman spectroscopy and scanning electron microscopy identified SWNTs mixed with cell debris in the black aggregates. The 266-cm<sup>-1</sup> Raman signal corresponded to aggregated SWNT bundles (20), whereas a broad photoluminescence peak observed ≈3,200 cm<sup>-1</sup> (≈1,050 nm) (Fig. 4*c*) corresponded to individual tubes also in existence. Scanning electron microscopy of the black aggregates after drying revealed tube-like strands stretched across cell debris or residues from the cell culture medium (Fig. 4*d* *Inset*). Cracks appeared in the nanotube-cell debris structures during drying, causing the aggregated bundles of nanotube to stretch across the cracks. Thus, we clearly observed that, accompanied by cell death, extensive NIR radiation caused molecular detachment or defunctionalization of SWNTs inside cells, leading to nanotube aggregation.

The result above hinted that if SWNTs can be selectively internalized into cancer cells with specific tumor markers, NIR radiation of the nanotubes *in vitro* can then selectively activate or trigger cell death without harming normal cells. This important goal prompted us to develop SWNT functionalization schemes with specific ligands for recognizing and targeting tumorous cell types. FRs are common tumor markers expressed at high levels on the surfaces of various cancer cells and facilitate cellular internalization of folate-containing species by receptor-mediated endocytosis (13). To exploit this system, we obtained highly water-soluble individualized SWNTs noncovalently functionalized by PL-PEG-FA (Fig. 5*a*). FR-positive HeLa cells (FR<sup>+</sup> cells) with overexpressed FRs on the cell surfaces were obtained by culturing cells in FA-depleted cell medium. Both FR<sup>+</sup> cells and normal cells without abundant FRs were exposed to PL-PEG-FA-SWNTs for 12–18 h, washed, and then radiated by a 808-nm laser (1.4 W/cm<sup>2</sup>) continuously for 2 min. After the NIR radiation, we observed extensive cell death for the FR<sup>+</sup> cells evidenced by drastic cell morphology changes (Fig. 5*b*), whereas the normal cells remained intact (Fig. 5*c*) and exhibited normal proliferation behavior over ≈2 weeks (Fig. 6), which was the

longest period monitored. The selective destruction of FR<sup>+</sup> cells suggested that PL-PEG-FA-SWNTs were efficiently internalized inside FR<sup>+</sup> cells (confirmed by fluorescence in Fig. 5*d* for SWNTs with FA cargo and FITC labels) and not inside normal cells (confirmed by the lack of fluorescence inside cells in Fig. 5*e*). The former was a result of selective binding of FA-functionalized SWNTs and FRs on FR<sup>+</sup> cell surfaces and receptor-mediated endocytosis. The latter was caused by the “inertness” or blocking of nonspecific binding of SWNTs imparted by the PEG moiety (6) on SWNTs and the lack of available FRs on the normal cells.

It is shown here that single-walled carbon nanotubes are molecular transporters or carriers with very high optical absorbance in the NIR regime where biological systems are transparent. This intrinsic property stems from the electronic band structures of nanotubes and is unique among transporters. Our current work exploits this property with a laser of  $\lambda = 808$  nm and can be extended to using light sources spanning the entire 700- to 1,100-nm range transparent to biosystems for more efficient *in vitro* excitations of SWNTs with various chiralities to obtain enhanced biological effects. NIR pulses can induce local heating of SWNTs *in vitro* for endosomal rupture and molecular cargo releasing for reaching intended targets without harming cells. On the other hand, selective killing of cells overexpressing tumor markers can be achieved by selective delivery of nanotubes inside the cells via receptor-mediated uptake pathways and NIR-triggered death. The scheme of SWNT functionalization by PEG ligands can be generalized to various ligands or antibodies targeting very specific types of cells. Although the PEG moiety imparts inertness and little nonspecific binding of nanotubes to normal cells, the ligands can recognize cells with complementary receptors for SWNT internalization and subsequent cell destruction by NIR radiation. Specifically functionalized nanotubes could then be a generic “killer” of various types of cancer cells without harming normal cells. Thus, the transporting capabilities of carbon nanotubes combined with suitable functionalization chemistry and the intrinsic optical properties of SWNTs can open up exciting new venues for drug delivery and cancer therapy. An alternative to endocytosis is directly injecting SWNTs into cells in selected tumor regions and then triggering tumor death by NIR radiation. Finally, we note that the only other NIR-absorbing nanomaterial that has been used for cell destruction is Au nanoshell by Halas, West, and coworkers (21) with a laser power of ≈4–35 W/cm<sup>2</sup> for >4 min. Our SWNT NIR agents compare favorably with lower laser power and shorter radiation times needed to effect cancer cell destruction because of high NIR absorbance of nanotubes. There is plenty of room for future exploration of various novel NIR nanomaterials for biological applications.

We thank Dunwei Wang for scanning electron microscopy analysis. This work was partly supported by the Stanford–National Science Foundation Center on Polymer Interfaces and Macromolecular Assemblies.

1. Henry, C. M. (2004) *Chem. Eng. News* **82**, 37–42.
2. Alivisatos, P. (2004) *Nat. Biotechnol.* **22**, 47–52.
3. Kim, S., Lim, Y. T., Soltesz, E. G., Grand, A. M., Lee, J., Nakayama, A., Parker, J. A., Mihaljevic, T., Laurence, R. G., Dor, D. M., *et al.* (2004) *Nat. Biotechnol.* **22**, 93–97.
4. Taton, T., Mirkin, C. & Letsinger, R. (2000) *Science* **289**, 1757–1760.
5. Cui, Y., Wei, Q., Park, H. & Lieber, C. (2001) *Science* **293**, 1289–1292.
6. Chen, R. J., Bangsaruntip, S., Drouvalakis, K. A., Kam, N. W. S., Shim, M., Li, Y., Kim, W., Utz, P. J. & Dai, H. (2003) *Proc. Natl. Acad. Sci. USA* **100**, 4984–4989.
7. Bianco, A., Kostarelos, K., Partidos, C. D. & Prato, M. (2005) *Chem. Commun.* **5**, 571–577.
8. Kam, N. W. S., Jessop, T. C., Wender, P. A. & Dai, H. J. (2004) *J. Am. Chem. Soc.* **126**, 6850–6851.
9. Cherukuri, P., Bachilo, S. M., Litovsky, S. H. & Weisman, R. B. (2004) *J. Am. Chem. Soc.* **126**, 15638–15639.
10. Dresselhaus, M. & Dai, H., eds. (2004) *MRS Bull. Adv. Carbon Nanotubes* **29**, 237–243.
11. König, K. (2000) *J. Microsc. (Oxford)* **200**, 83–104.
12. O’Connell, M. J., Bachilo, S. M., Huffman, C. B., Moore, V. C., Strano, M. S., Haroz, E. H., Rialon, K. L., Boul, P. J., Noon, W. H., Kittrell, C., *et al.* (2002) *Science* **297**, 593–596.
13. Lu, Y. J., Segal, E., Leamon, C. P. & Low, P. S. (2004) *Adv. Drug Delivery Rev.* **56**, 1161–1176.
14. Nikolaev, P., Bronikowski, M. J., Bradley, R. K., Rohmund, F., Colbert, D. T., Smith, K. A. & Smalley, R. E. (1999) *Chem. Phys. Lett.* **313**, 91–97.
15. Zheng, M., Jagota, A., Semke, E. D., Diner, B. A., McLean, R. S., Lustig, S. R., Richardson, R. E. & Tassi, N. G. (2003) *Nat. Mater.* **2**, 338–342.
16. Bachilo, S. M., Strano, M. S., Kittrell, C., Hauge, R. H., Smalley, R. E. & Weisman, R. B. (2002) *Science* **298**, 2361–2366.
17. Mukherjee, S., Ghosh, R. N. & Maxfield, F. R. (1997) *Physiol. Rev.* **77**, 759–803.
18. Cho, Y. W., Kim, J. D. & Park, K. (2003) *J. Pharm. Pharmacol.* **55**, 721–734.
19. Boussif, O., Lezoualc’h, F., Zanta, M. A., Mergny, M. D., Scherman, D., Demeneix, B. & Behr, J. (1995) *Proc. Natl. Acad. Sci. USA* **92**, 7297–7301.
20. O’Connell, M. J., Sivaram, S. & Doorn, S. K. (2004) *Phys. Rev. B* **69**, 235415–1–15.
21. Hirsch, L. R., Stafford, R. J., Bankson, J. A., Sershen, S. R., Rivera, B., Price, R. E., Hazle, J. D., Halas, N. J. & West, J. L. (2003) *Proc. Natl. Acad. Sci. USA* **100**, 13549–13554.